

# Human Inspired Autonomous Intersection Handling Using Game Theory

Keqi Shu<sup>1</sup>, Graduate Student Member, IEEE, Reza Valiollahi Mehrizi, Shen Li<sup>1</sup>, Member, IEEE,  
Mohammad Pirani<sup>1</sup>, Member, IEEE, and Amir Khajepour<sup>1</sup>, Senior Member, IEEE

**Abstract**—Left turning for autonomous vehicles at intersections is challenging due to the various driving behaviors from different human drivers and the strong interaction between the autonomous vehicle and human traffic participants. This paper proposes a planning and decision making framework for intersection left-turning which considers the interaction between autonomous vehicles and human drivers as well as pedestrians to address this issue. The proposed framework considers interactions mathematically by formulating the problem as a linear quadratic differential game. Through solving the Nash equilibrium of the game, the autonomous vehicle is able to properly interact with surrounding traffic participants. Under the differential game framework, the accuracy of the interaction formulation is closely related to the behavior model of human drivers. Therefore, real-world human behavior is extracted and evaluated from naturalistic driving dataset to help establish more realistic modeling and estimation of various kinds of traffic participants, including aggressive, neutral and conservative traffic participants. The simulation results show that the autonomous vehicle is able to properly estimate the types of traffic participants by observing their behavior using the proposed technique. Then the autonomous vehicle behave according to the types of those traffic participants to enable interactive and human-like planning and decision making at intersections.

**Index Terms**—Autonomous vehicles, intersection handling, decision making, planning, game theory, real-world data.

## I. INTRODUCTION

### A. Background

PLANNING and decision-making of autonomous vehicles have been widely developed in academia and industry. Decision-making plays as one of the most challenging part when autonomous vehicles interact with human [1]. Complicate traffic system structure and traffic rules add to this challenge. Hence, safe interaction between the human and autonomous vehicles becomes crucial in decision-making tasks.

One of the above-mentioned interaction scenario which is very common in daily driving is intersection scenario. Over

Manuscript received 28 November 2022; revised 19 April 2023; accepted 17 May 2023. Date of publication 12 June 2023; date of current version 4 October 2023. The Associate Editor for this article was Y. Wiseman. (Corresponding author: Keqi Shu.)

Keqi Shu, Reza Valiollahi Mehrizi, Mohammad Pirani, and Amir Khajepour are with the Department of Mechanical and Mechatronics Engineering, University of Waterloo, Waterloo, ON N2L 3G1, Canada (e-mail: k3shu@uwaterloo.ca).

Shen Li is with the Department of Civil Engineering, Tsinghua University, Beijing 100084, China.

Digital Object Identifier 10.1109/TITS.2023.3281390

40% of all injury accidents occur at intersections in the USA [2]. As for autonomous vehicles, most decision-making and planning algorithms could not guarantee 100% safety because of the complex and quickly-evolving characteristics of intersection scenarios [3].

Among all the intersection decision-making and planning scenarios, left-turning is one of the most critical one. Where interaction among the autonomous vehicle and the surrounding vehicles are very strong due to the rapid-changing right-of-way and states. Without the help of a centralized traffic management system [4], it is a challenging task to estimate the future states of the surrounding vehicles correctly and, at the same time, be able to behave accordingly.

### B. Literature Review

In the literature, researchers try to solve the intersection handling problems by considering interaction behaviours as one-way or bi-directional interaction [5].

One-way interaction approaches consider the oncoming vehicle or pedestrians as obstacles and only consider their influence on the autonomous vehicle, while the ego vehicle behaves passively [6]. One popular approach is the network-based reinforcement learning methods [7]. Li et al. proposed inverse reinforcement learning (IRL) to perform defensive driving at intersections. The heuristics are represented by deep Q-networks trained from real-world data [8]. Hu et al. proposed a deep-IRL framework that improves the generalization and effectiveness of dealing with corner cases [9]. However, this approach performs less outstanding in scenarios where driving data is not covered, and needs to consider the influence of the ego vehicle on the surrounding traffic participants.

The bi-directional interactive decision-making and planning approaches enable the autonomous vehicles not only trying to keep safe distances according to the surrounding traffic participants' behaviours, but at the same time, consider their own behaviour's influence on the surrounding vehicles' strategies. This type of modelling will help the autonomous vehicle to better estimate the current scenario and make sound decisions. Among all the decision-making frameworks that consider bi-directional interactive behaviours, one of the most popular approach is the game-theory-based framework.

One classical game theory-based decision-making model is the Stackelberg game [10], [11]. This formulation assumes

that two players follow certain priority rules, for example, the right-of-way of vehicles. Li et al. [12] formed the vehicles with leader-follower pairs based on common traffic rules. Reference [13] applied Stackelberg game modelling to enable better unprotected left turns at intersections. These kinds of methods are commonly applied in merging or lane-changing scenarios [14], [15], where the right-of-way is clear, and the interaction is usually simple. However, is less applicable in strong-interactive scenarios.

Another trendy method is the level-k game method [16]. This method finds the Nash equilibrium by updating each player's strategy iteratively and sequentially. Reference [17] applied level-k algorithm in uncontrolled intersection handling with vehicles violating traffic rules. Li et al. [18] also applied a level-k time-extended, multi-step, and interactive decision-making framework that operates at uncontrolled intersections. However, these algorithms still solve the problem in a discrete action space and suffer from the curse of dimensions.

To realise intersection handling under continuous space, the feedback-loop differential game framework was introduced. This framework expresses the time-inconsistent interaction behaviour in a theoretical way and convert the game into an optimization problem [19]. Fridovich-Keil et al. proposed an iterative linear quadratic differential game framework which decreased the computational time for finding the Nash equilibrium by linearizing the problem and setting the optimization functions in a quadratic format [20]. They also solved the problem by projecting the states of the problem to the linearized system space to increased the convergence rate [21]. The closed feedback-loop differential game showed promising results in simulations due to its exceptional ability in representing interaction behaviours in an expressive way. However, the previous works assume perfect modelling of the surrounding traffic participants' behaviours. The behaviour model of surrounding traffic participants and the way they interact with each other were set up through driving experience or common sense as a uniform format. In the real world, however, human behaviour does not generate from a uniform model and people usually have different "heuristics." These issues make the implementation of feedback-loop differential game in the real world less ideal (optimal) than in simulation.

Numerous driver models have been proposed to represent interaction behaviours at intersections accurately. One popular approach is to use neural networks to model driver behaviour. For instance, Xu et al. used large-Scale video datasets to train the black-box driver model [22]. Peng et al. also proposed a back-propagation neural network driver behaviour model to improve the accuracy of the modelling [23]. However, these models heavily rely on the comprehensiveness of the dataset and may be difficult to tune for specific drivers.

Other approaches simulate driver behaviours at intersections by proposing parameterized and adaptable driver models. For example, [24] extended the classical Intelligent Driver Model (IDM) [25] into a more generalized format by considering surrounding traffic participants' interaction behaviours. Xin et al. proposed a predictive IDM based on V2X communication to reduce idling time at signalized intersections [26]. These methods could be more accurate than a black-box driver

model but the interactive behaviours might not be fully represented.

### C. Contributions

To overcome the aforementioned problems in the literature, this paper proposes a decision-making framework for intersections handling based on the feedback-loop linear quadratic game algorithm. Naturalistic real-world driving data is used to help analytically represent more realistic interaction behaviours between the ego vehicle and surrounding traffic participants. This enable autonomous vehicles to find more applicable and natural solutions in real life.

The contributions of our paper are as follows:

- we introduced a novel algorithm for intersection handling that employs game theory and realistic driving characters extracted from naturalistic driving data, thus promoting efficiency and reliability under high-interactive scenarios;
- we developed a traffic participant's driving character estimation model, which enables the autonomous vehicle to infer the driving characters from observing critical features extracted from driving data in real-time and make sound decisions accordingly;
- our approach enhances the computational efficiency of uncertain driving character estimation and interactive game-based decision-making in continuous action spaces, enabling real-time performance.

Our proposed framework represents improvements over existing literature in intersection handling, particularly in the following aspects. The proposed framework accounts for bi-directional interaction, specifically how the ego vehicle's possible behaviours can influence surrounding vehicles. A realistic driver model was extracted from a naturalistic driving dataset with a high level of interaction, which accurately represents the bi-directional interaction feature in the driver model. The proposed uncertain driver character estimation model integrates the extracted driver model into a game-based decision-making framework. This allows the autonomous vehicle to interact appropriately with different types of drivers. Furthermore, the relationship between the critical observation feature and driving character was extracted from real-world data. By linearizing the problem and utilizing the character estimation model, our framework reduces the computational load, allowing the ego vehicle to find a solution in real time for a continuous action space with various traffic participants.

## II. INTERSECTION INTERACTIVE LEFT-TURNING DECISION MAKING FRAMEWORK

The overall decision-making framework is presented in Fig. 1. Where sub-figure (a) is one typical scenario that the framework could be implemented, that is, a left-turning autonomous vehicle tries to cross the intersection with two different human-driven vehicles potentially blocking the way. The red vehicle (AV1) is the autonomous vehicle and the other two blue vehicles are the human-driven vehicle labelled as HV1 and HV2. The colour bars in the yellow bounding boxes help indicate the driving style of the human drivers. The arrow pointing more on the yellow side indicates that the driver is

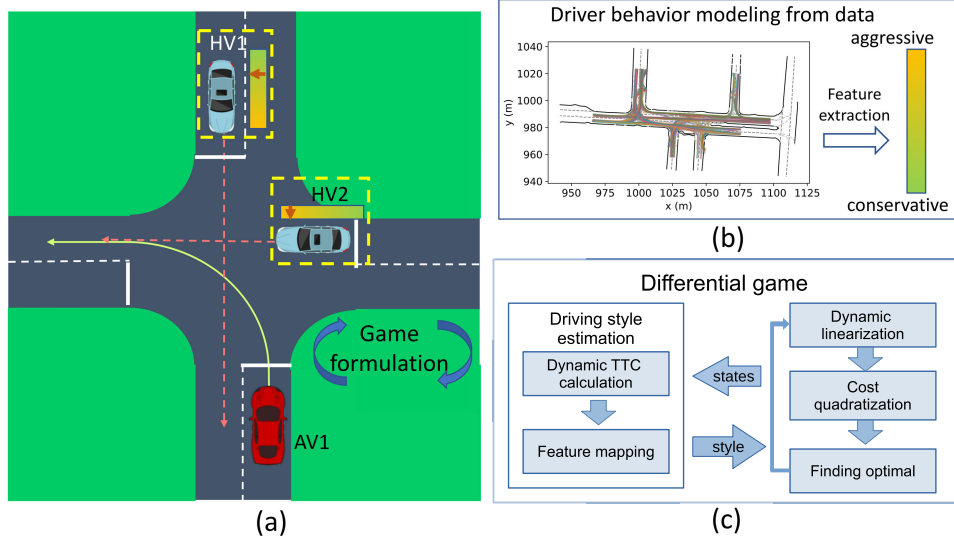


Fig. 1. Naturalistic autonomous intersection handling framework.

more aggressive and wise versa. The red dashed lines are the nominal paths of the human-driven vehicle and the green dashed polynomial is the nominal path of the ego vehicle.

To help the autonomous vehicle to make proper decisions considering the interactions with human-driven vehicles, the human-driver models are carefully modified. A naturalistic intersection driving dataset [27] had been used to extract realistic human behaviours. As shown in Fig. 1 (b), the data was used to extract features of different human drivers and then properly set up the driving style.

Given the modified driver models and the features of various kinds of human drivers, it is possible to consider different drivers when making decisions. Based on an analysis of real-world driving scenarios and driving datasets, it was discovered that the decision-making process is complicated by the unpredictable driving styles of surrounding drivers and rapidly changing situations. Thus, the framework is designed to enable the ego vehicle to continuously assess the human driver's behaviour and make appropriate decisions in real-time.

This function is demonstrated on the left-hand side of Fig. 1 (c), where the driving style is estimated through the dynamic time to collision (TTC) calculated from the latest states of all the traffic participants. The dynamic TTC includes the derivative of the TTC and the TTC itself. After the driving style is estimated in real-time, the data-extracted features of the utility function that represents various driving styles are updated, and used to solve the differential game.

Given the up-to-date information on the surrounding human-driven vehicles and also the environment, the ego vehicle would be able to solve the decision-making problem accordingly. The ego vehicle formulates the interaction between the traffic participants in a mathematical and analytical way using a differential game framework. By transferring the game into an optimization problem, the Nash equilibrium of the game could be found by finding the optima.

The differential game formalization of the ego vehicle is demonstrated on the right-hand side of Fig. 1 (c). To improve

the computational efficiency in the nonlinear system, the framework linearizes the players' dynamics and formulates costs in quadratic form. This approach enables real-time solution finding, but the linearized solution is only valid when the states do not deviate significantly from the current states. To obtain a solution for the original problem, the solver considers the possible future states of all players and iteratively searches for a better solution with small steps until it is close enough to the Nash equilibrium.

This differential-game-based intersection handling algorithm works in a receding horizon format, that the ego vehicle makes a decision at each time step considering the actions of other traffic participants of a fixed time horizon. Which makes the proposed framework more applicable.

### III. ITERATIVE LINEAR QUADRATIC DIFFERENTIAL GAME FORMULATION AND SOLVING

To allow the autonomous vehicle to make proper left-turning decisions in the high-interactive scenario. A framework based on iterative linear quadratic differential game that analytically formulates the interaction into the decision-making process was implemented. It tries to reach the best result given the nominal paths of each traffic participant as well as each traffic participant's heuristics. The formulation and the game solving method will be explained in further detail in this section.

#### A. Game Formulation

1) *Dynamics and Utility Functions of Players:* the first step in the game formulation is setting up the dynamics of the players in the intersection scenario which include vehicles' and pedestrians' dynamics. For autonomous vehicles and human-driven vehicles, a 5-D kinematic model is implemented. The states of the vehicles are  $(x, y, v, \theta, \phi)$ .  $x$  and  $y$  are the Cartesian positions of the vehicles,  $v$  is the speed,  $\theta$  is the heading angle, and  $\phi$  is the steering angle of the vehicle. The dynamics

of the vehicles could be demonstrated as follows:

$$\begin{cases} \dot{x} = v \cos \theta \\ \dot{y} = v \sin \theta \\ \dot{\theta} = (v \tan \phi)/l \\ \dot{\phi} = u_1 \\ \dot{v} = u_2, \end{cases} \quad (1)$$

where  $u_1$  and  $u_2$  are the inputs of the vehicle, that is, the inputs are the steering rate and acceleration. The inputs of the vehicles can be expressed as  $u = (u_1, u_2)$

For pedestrians, due to the all-directional moving nature and the smaller size, the kinematic model is simplified as a point-mass model in which the states of the pedestrian could be expressed as  $x, y, v, \theta$ , that  $x$  and  $y$  are the positions and  $v$  and  $\theta$  are the velocity and the humans' facing-direction angle accordingly. Thus the dynamics for pedestrians are:

$$\begin{cases} \dot{x} = v \cos \theta \\ \dot{y} = v \sin \theta \\ \dot{\theta} = u_1 \\ \dot{v} = u_2, \end{cases} \quad (2)$$

where the inputs  $u_1$  and  $u_2$  are the turning rate and acceleration accordingly.

The next step is to set up proper behaviour models for the players in the game. To analytically formulate the behaviours of the players, various features have been used in the utility functions. For vehicles, including autonomous vehicles and human-driven vehicles, the utility functions are defined as the affine combination of different heuristics as:

$$g_i(t, x(t), u_{1:N}(t)) = [K_{safe}, K_{nom}, K_{comf}] \begin{bmatrix} R_{safe} \\ R_{nom} \\ R_{comf} \end{bmatrix}, \quad (3)$$

where  $g_i(\cdot)$  represents the utilities of the  $i$ th traffic participant. The features of the vehicles could be divided into three main categories: the safety feature  $R_{safe}$ , the nominal path and speed feature  $R_{nom}$ , and the riding comfort feature  $R_{comf}$ .  $K_{(\cdot)}$  is the coefficient of each of these features. These features with their coefficients together describe how a vehicle would behave in a given scenario. A more detailed description of the features is described as follows.

The safety feature  $R_{safe}$  could be expressed as:

$$R_{safe} = \begin{bmatrix} R_d \\ R_g \end{bmatrix}, \quad (4)$$

where  $R_d$  is the heuristic such that vehicles need to keep a minimum safe distance from all other traffic participants, and  $R_g$  is the accepted gap feature to ensure the left-turning vehicle has enough time and space to make the left turn. More specific explanation of  $R_d$  and  $R_g$  are made as follows.

The minimum distance heuristic  $R_d$  could be written as:

$$R_d = \sum_{j=1}^{N-1} \begin{cases} 0 & \text{if } dis(p_i, p_j) \geq d_m \\ (d_m - dis(p_i(x, y), p_j(x, y)))^2 & i \neq j, \\ & \text{if } dis(p_i, p_j) < d_m \end{cases} \quad (5)$$

where  $p_i = (x_i, y_i)$  and  $p_j = (x_j, y_j)$  are the positions of the ego vehicle and the traffic participants around it in the Cartesian space.  $N$  is the total number of players in the intersection scenario, where  $j$  indicates any traffic participant around traffic participant  $i$ .  $d_m$  stands for the minimum distance between the vehicle and the other traffic participants.  $dis(\cdot)$  represents the distance between the two traffic participants. If  $dis(\cdot)$  is smaller than the safety distance  $d_m$ , then an exponential cost will be assigned to the vehicle.

The minimum gap feature  $R_g$  is also a safety feature, which ensures the left-turning ego vehicle maintains a "turning-safe" gap with the oncoming vehicle. This safe gap is the  $l^1$ -norm distance between the left-turning vehicle and the oncoming vehicle in the oncoming vehicle's 1D direction, which is proposed inspired by the accepted gap concept [28]. The  $d_g$  is positively proportional to the oncoming vehicle's speed, and a penalty is given if the  $l^1$ -norm safe gap is smaller than  $d_g$ .

The nominal speed and path feature  $R_{nom}$  could be expressed as:

$$R_{nom} = \begin{bmatrix} R_s \\ R_l \end{bmatrix}, \quad (6)$$

where  $R_l$  and  $R_s$  are the heuristics for keeping the traffic participants moving along the nominal path with the nominal speed profile.  $R_l$  could be expressed as:

$$R_l = \begin{cases} k_n |proj(p_i(x, y), l_{poly})|, & \text{if } dis(p_i(x, y), l_{poly}) < l_b \\ k_b(proj(p_i(x, y), l_{poly}) - l_b)^2, & \text{if } dis(p_i(x, y), l_{poly}) \geq l_b, \end{cases} \quad (7)$$

where  $l_{poly}$  represents the polynomial nominal trajectory that is generated using road geometry.  $l_b$  is half of the road width.  $proj(\cdot)$  is a distance projection function that calculates the closest distance from the vehicle's planned future trajectory to the center line of the given nominal path. Finally,  $k_n$  and  $k_b$  are constants which scale the utilities.  $R_l$  is designed to provide a huge penalty for vehicles that are off the road and a relatively small penalty for off-setting from the nominal path. Therefore,  $k_b$  shall be much larger than  $k_n$ .

$R_s$  is designed for the vehicle to follow the nominal speed and does not violate speed limits. This heuristic could be expressed as:

$$R_s = \begin{cases} k_m^v (s_v - s_{max})^2, & \text{if } s_v > s_{max} \\ k_n^v |s_v - s_n|, & \text{if } 0 \leq s_v \leq s_{max} \\ k_i^v (s_v)^2, & \text{if } s_v < 0, \end{cases} \quad (8)$$

where  $s_v$  is the current speed of the ego vehicle,  $s_{max}$  is the speed limit of the intersection and  $s_n$  is the nominal speed profile of the vehicle.  $k_m^v$ ,  $k_n^v$  and  $k_i^v$  are constant ratio. The heuristics are designed to give a huge penalty if the vehicle is driving over the speed limit or going backwards, therefore,  $k_m^v$  and  $k_i^v$  are relatively much larger than  $k_n^v$ .

Finally, a smooth feature is defined as  $R_{comf}$ , which represents the behaviour of drivers tended to accelerate, decelerate and steer as less as possible. The expression of this feature is:

$$R_{comf} = \begin{bmatrix} R_a \\ R_w \end{bmatrix}, \quad (9)$$

where

$$R_{a/w} = (a/w)^2. \quad (10)$$

$a$  and  $w$  are the acceleration and steering angle of the vehicle.

Since the driving behavior features  $R_{safe}$ ,  $R_{nom}$  and  $R_{comf}$  are written in an array format. The coefficients of the features:

$K_{safe}$ ,  $K_{nom}$ ,  $K_{comf}$  are also in a array format:  $K_{safe} = [K_d, K_g]^T$ ,  $K_{nom} = [K_s, K_l]^T$ , and  $K_{comf} = [K_a, K_w]^T$ .

For pedestrians behaviour modelling, the features are similar to the vehicle's modelling which also have utilities in three aspects,  $R_{safe}^P$   $R_{nom}^P$  and  $R_{comf}^P$ . However, there are still some minor differences. For  $R_{safe}^P$ , the minimum gap  $R_g^P$  is not considered. For  $R_{comf}^P$ , since a point-mass model is being implemented for the pedestrians modelling, instead of considering minimizing acceleration and steering angle, this model considers minimizing the acceleration in the  $x$  and  $y$  axis. Finally, similar to driver's utility function (3),  $K_{(\cdot)}^P$  is the coefficient of the pedestrians' features.

2) *Dynamic Linearization and Costs Quadratization*: subsection III-A1 describes the state space and action space of traffic participants and their behaviour heuristics. This subsection describes how to transfer the problem into a differential game.

The nonlinear dynamics of the players is:

$$\dot{s}(t) = f(s(t), u_{1:N}(t)), \quad (11)$$

where  $s(t)$ ,  $u_{1:N}(t)$  are the state and inputs of each traffic participant accordingly at time  $t$ . This nonlinear formulation makes the dynamics model closer to reality but increase the computational load. To improve real-time performance, the dynamics needs to be linearized.

This linearization is realised through making a Jacobian linearization [29] over the offsets of arbitrary states and inputs to the nominal ones:

$$\dot{\delta}_s(t) = A(t)\delta_s(t) + \sum_{i \in N} B_i(t)\delta_u(t), \quad (12)$$

where the offset is  $\delta_s(t) = s(t) - \bar{s}(t)$  and  $\delta_u(t) = u(t) - \bar{u}(t)$ ,  $\bar{s}$  and  $\bar{u}$  represent the nominal states and inputs. The dynamic matrices could be expressed as  $A = \frac{\partial f}{\partial s} \Big|_{\substack{x=\bar{s} \\ u=\bar{u}}} \in \mathbf{R}^{n \times n}$  and

$$B_i = \frac{\partial f}{\partial u_i} \Big|_{\substack{s=\bar{s} \\ u=\bar{u}}} (t) \in \mathbf{R}^{n \times m}.$$

It is demonstrated in [29] that when  $\delta_s$  and  $\delta_u$  is "small" enough, the linearization holds. Without the loss of generality and to make the problem easier to handle, the system is discretized, where the states  $s$  transfer from time step  $k$  to  $k+1$ . Now, the new "A" is " $A^* = e^{AT}$ " and the new "B" is  $B^* = A^{-1}(e^{AT} - \mathbf{I})\mathbf{B}$ .

The next major procedure to increase the real time performance is converting the cost into quadratic form. Given the heuristics of each player presented in subsection III-A1, the quadratic approximation of the cost could be rewritten as:

$$\begin{aligned} & g(s + \delta s, u_{1:N}(k) + \delta u_{1:N}(k), k) - g(s, u_{1:N}(k), k) \\ & \approx \frac{1}{2}\delta s(k)^T Q_i(k)\delta s(k) + \delta s(k)^T l_i(k) \\ & + \frac{1}{2} \sum_{j \in N} \delta u_j(k)^T (R_{ij}(k)\delta u_j(k) + 2r_{ij}(k)). \end{aligned} \quad (13)$$

Given  $g_i$  represents the utility functions of the traffic participants, some variable is the first partial derivable of  $g_i$ :  $l_i = \frac{\partial g_i}{\partial s}$ ,  $r_{ij} = \frac{\partial g_i}{\partial u_j}$ , and some are the Hessian:  $Q_i = \frac{\partial^2 g_i}{\partial s \partial s}$  and  $R_{ij} = \frac{\partial^2 g_i}{\partial u_j \partial u_j}$ . The  $L$ ,  $Q$ ,  $R$  matrices are obtained to solve the linear quadratic differential game.

### B. Solving the Game

After the linear approximated dynamic system and the quadratic approximated cost is obtained, the modified problem now follows the definition of a differential game. In other words, it is possible to be transformed into an optimization problem. The Nash equilibrium of the game could then be calculated by finding the optima iteratively [20].

The problem is assumed to follow a feedback information structure, where the optima is in the following format [20]:

$$\delta u_i^*(k) = -P_i^*(k)\delta s(k) - \delta \alpha_i^*(k), \quad (14)$$

where  $\delta u_i^*(k) = \tilde{\gamma}_i^o(k, s(k)) - \hat{u}_i(k)$ , and  $\tilde{\gamma}_i^o(k, s(k))$  represents the feedback strategy generated for player  $i$  after  $o$ th iteration to come to a feedback Nash equilibrium. The feedback parameter  $P_i(k)$  are matrices with size  $m_i \times n$  and  $\alpha_i(k)$  is the additional term. These variables can be calculated by solving (15) and (16) assuming strong convexity [30]. The two sets of equations are obtained by setting the gradients of the quadratic utility functions to zero:

$$\begin{aligned} & \left( R_{ii}^o + B_i^{oT} Z_i^{o+1} B_i^o \right) P_i^o + B_i^{oT} Z_i^{o+1} \sum_{j \neq i} B_j^o P_j^o \\ & = B_i^{oT} Z_i^{o+1} A^o, \end{aligned} \quad (15)$$

$$\begin{aligned} & \left( R_{ii}^o + B_i^{oT} Z_i^{o+1} B_i^o \right) \alpha_i^o + B_i^{oT} Z_i^{o+1} \sum_{j \neq i} B_j^o \alpha_j^o \\ & = B_i^{oT} \zeta_i^{o+1}. \end{aligned} \quad (16)$$

$R_{ii}^o$  is the Hessian matrix after  $o$ th iteration calculated in (13) and  $Z_i^o$  can be calculated recursively by:

$$Z_i^o = F^{oT} Z_i^{o+1} F^o + \sum_{j \in N} P_j^{oT} R_{ij}^o P_j^o + Q_i^o, \quad (17)$$

where  $Z_i^{o+1} = Q_i^{o+1}$ , ( $i \in \mathbf{N}$ ) and  $F^o \triangleq A^o - \sum_{i \in N} B_i^o P_i^o$  ( $k \in \mathbf{O}$ ).  $O$  is the total number of iteration.  $\zeta_i^o$  ( $i \in \mathbf{N}$ ) can also be calculated by recursively solving:

$$\zeta_i^o = F^{oT} \left( \zeta_i^{o+1} + Z_i^{o+1} \beta^o \right) + \sum_{j \in N} P_j^{oT} R_{ij}^o \alpha_j^o, \quad (18)$$

where  $\zeta_i^{o+1} = 0$ ,  $i \in \mathbf{N}$  and  $\beta^o \triangleq c^o - \sum_{j \in N} B_j^{oT} \alpha_j^o$  ( $k \in \mathbf{K}$ ). Finally, the Nash equilibrium of the game could be found using (14) given the calculated  $P_o^i(k)$  and  $\alpha_o^i(k)$ .

### IV. REALISTIC BEHAVIOURAL MODELLING AND ESTIMATION

In the proposed framework, the autonomous vehicle makes decisions on the assumption of how the other traffic participants might behave given their behaviour models. To achieve good performance of the framework, a realistic interactive behavioural model and its estimation model are proposed.

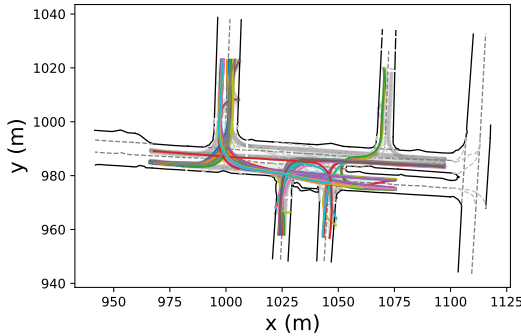


Fig. 2. Human driving behavior extracted from the naturalistic intersection driving dataset.

#### A. Behavior Model Extraction From Naturalistic Data

In the real world, the kinds of traffic participants are very diverse and show different level of aggressiveness. This could be presented in the proposed behavioural model by setting the features that distinguish various kinds of behavioral styles. Which include the safety gaps  $d_m$  in (5), the nominal speed  $s_n$  in (8) and the coefficient parameters  $K_{(.)}$ . All these parameters change continuously accordingly to various driving style.

To present realistic behavior model, a naturalistic INTERACTION dataset [27] was used to extract the aforementioned parameters. However, some of the features are subjective such as the coefficient characters  $K_{(.)}$ , which is implicitly presented in the dataset. Therefore, only the objective features such as  $d_m$ ,  $d_g$ ,  $s_n$ , etc. are extracted from the dataset.

An intersection scenario with rich interaction behaviors in the dataset is selected and is demonstrated in Fig. 2. The black lines indicate the boundaries of the road and the dashed lines are the interior boundaries and the guided lines of the lanes. The coloured lines and the gray lines are all the trajectories of the vehicles in the scenario. A significant difference between this figure and Fig. 1 is that all the left-turning trajectories are highlighted with coloured lines in this figure, and all the rest of the trajectories are plotted in gray. The features extracted from the dataset include non-interactive and interactive features. The non-interactive features are the nominal features such as the nominal speed. The interactive behaviour features includes minimum distance between the traffic participants, and the accepted gap between the left-turning vehicle and the oncoming vehicle, etc.

*1) Non-Interactive Behaviours Extraction and Analysis:* One important feature of non-interactive behaviours is nominal speed. The left-turning and oncoming vehicles' trajectories were extracted and presented as coloured trajectories in Fig. 2.

The nominal speed is extracted from non-interactive behaviours, therefore, interactive left-turning trajectories are filtered out from the dataset. A bold but rational assumption is made that the non-interactive drivers dose not perform hard braking. For example, if a scenario has a left-turning vehicle whose deceleration is larger than  $2.5 \text{ m/s}^2$ , then this is an interactive scenario.

After filtered out the non-interactive behaviours, the speed profiles along all the left-turning trajectories are obtained and presented in Fig. 3. Where the speed profiles are plotted

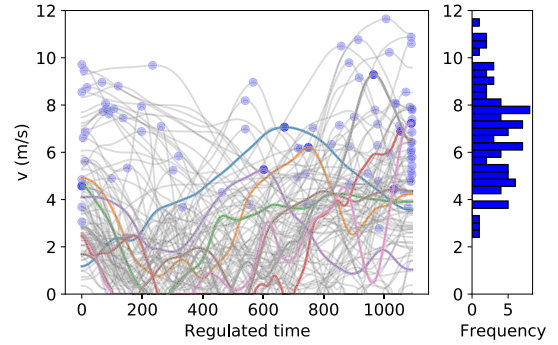


Fig. 3. Speed profile of left-turning trajectories and the maximum speed distribution.

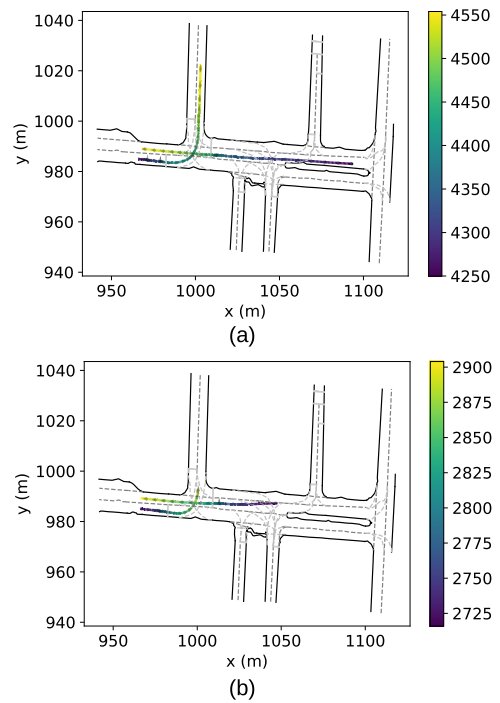


Fig. 4. Typical interactive left-turning scenarios: (a) left-turning vehicle passes the intersection first; (b) oncoming vehicle passes the intersection first.

according to time, and are regulated to the same time frame. The grey lines and the colour lines in the left sub-figure of Fig. 3 are the speed profiles according to time, the blue scattered dots are the maximum speed of the speed profile. Which would be the nominal speed of the vehicles.

The right-hand side sub-figure of Fig. 3 is the distribution of the maximum speed of the left-turning behaviors, the figure shows that the nominal speed various from  $3 \text{ m/s}$  to over  $12 \text{ m/s}$  and majorly lies under the  $4 \text{ m/s} - 8 \text{ m/s}$  range. The oncoming speed profile are extracted under the same way and the speed various from  $5 \text{ m/s}$  to  $12 \text{ m/s}$  and majorly falls in the  $6 \text{ m/s} - 10 \text{ m/s}$  range.

*2) Interactive Behaviours Extraction and Analysis:* The interactive left-turning behaviours were extracted from left-turning scenarios which is presented in Fig. 4. The two polynomials are the trajectories of the drivers, and the colour along the trajectories indicates the time information of the trajectories, where the colour bars on the right are the time

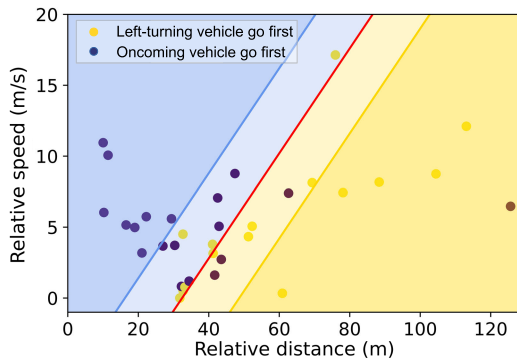


Fig. 5. Relative distance and speed of left-turning vehicle and oncoming vehicle at turning-decision point.

frame indicator with the unit as *ms*. The pointers along the trajectory's polynomials indicate the direction that the vehicle is driving.

Fig. 4 (a) and (b) are typical intersection left-turning scenarios, which are left-turning and oncoming vehicle passes the intersection first accordingly. All the related information such as the vehicles' speed, acceleration, heading angle, etc. are extracted from all these scenarios.

The decision-making points are extracted from the scenarios, defined as the places where the left-turning vehicle starts to accelerate or decelerate before the heading angle starts to change to the left. The states information of these decision-making points is processed and presented in Fig. 5, which are the relative distance and speed between the ego vehicle and the oncoming vehicle.

The yellow and blue colours correspond to scenarios of left-turning or oncoming vehicles passing the intersection first accordingly. The deep-blue shaded area is where most left-turning vehicles yield to the oncoming vehicle, and the deep yellow shaded area is where most left-turning vehicles make the left turn first. The light-coloured middle area is where both behaviours happen. The figure showed that the dataset includes rich and well-distributed interaction scenarios. As proposed in section IV, the accepted time gap is one of the major indicators of the driver's behaviour style. Therefore, the left-turning and oncoming trajectory sets are extracted and the time difference between the two vehicles to reach the potential collision point (also known as the TTC) are calculated and presented in Fig. 6. The orange bars represent the case when the left-turning vehicle yield to the oncoming vehicle and the blue bars represent the case where the oncoming vehicle yield to the left-turning vehicle. It can be seen that a left-turning vehicle would make a left turn before the oncoming vehicle if the time gap is around 10 s ( $\pm 3$  s) or larger. When the time gap is less than 4 s the left-turning would yield, and if the gap is between 4 s - 8 s, the two kinds of driving behaviours both occur. This figure demonstrated that different drivers would accept various minimum time gaps, which nicely represents the driving style of different drivers. Another very important interactive feature is the minimum distance that each vehicle keeps between other vehicles. Which is also a key representation of different kinds of drivers. All the scenarios with vehicles' relative distance less than a certain

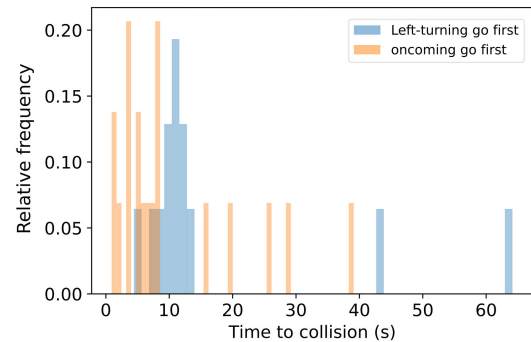


Fig. 6. Left-turning time gap distribution.

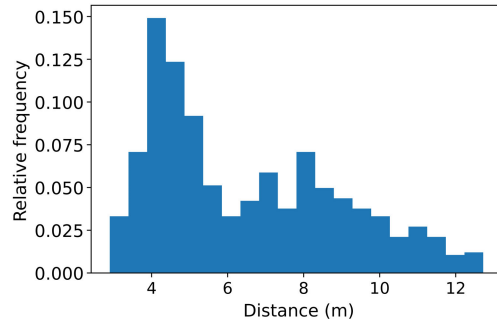


Fig. 7. Traffic participants' minimum distances distribution.

value (in this case 13 meters) are extracted. Then the minimum distances of these scenarios are extracted and their distribution are presented in Fig. 7. Where the x-axis is the minimum distance value, and the y-axis indicates the distribution. The figure showed that most vehicles keep a minimum distance of around 4 meters to 9 meters.

### B. Behavior Model Estimation

The proposed behavioral model allows the planning and decision making framework represent various kinds of driving styles. However, in the real-world application, traffic participants do not know the driving style of each other. Therefore the autonomous vehicle has to properly estimate the driving style of other traffic participants to enable sound interaction.

One very distinct feature that indicates different kinds of drivers is the accepted time gap (TTC). For example, if one left-turning vehicle makes a left turn under a 5-second gap, and another vehicle yields to the oncoming vehicle under a 5-second gap, then the first vehicle is more aggressive than the second vehicle. This also works for the oncoming vehicle.

Therefore, two features that are closely related to the accepted time gap *TTC* are considered for driving style estimation. The autonomous ego vehicle takes in the speed and positions of the surrounding traffic participants, and calculates the *TTC*, then makes an estimation based on this feature as:

$$M_s = k_t t_{ttc} + k_i \dot{t}_{ttc} \quad \text{if } t_{min} < t_{ttc} < t_{max}, \quad (19)$$

where  $M_s$  is the estimated driving style,  $t_{ttc}$  and  $\dot{t}_{ttc}$  are the *TTC* and the change of *TTC* respectively,  $k_t$  and  $k_i$  are the constant coefficients,  $t_{max}$  and  $t_{min}$  are the estimation threshold of the *TTC*. If the *TTC* is out of the estimating range (too small

TABLE I  
INTERVALS OF DRIVING CHARACTERS FOR VARIOUS DRIVERS

	Aggressive	Neutral	Conservative
$d_m$ (m)	< 5	5 - 9	> 9
$\frac{d_g}{v_{oncome}}$ (s)	< 4	4 - 8	> 8
$s_n$ (m/s)	< 6	6 - 10	> 10

or too large), e.g. if the TTC is too small, then no matter what the driver's character is, the autonomous vehicle needs to yield to the human driver.

Thus, the autonomous vehicle only estimates the human driver's driving style if  $t_{ttc} \in (t_{min}, t_{max})$ . Which decreases the computational load of the algorithm. The value of  $M_s$  decides the aggressiveness of the human driver, the smaller the value is, the more aggressive the driver is, and vice versa. For example, if the TTC ( $t_{ttc}$ ) is very large, and is increasing ( $\dot{t}_{ttc} > 0$ ) throughout the left-turning process, which means  $M_s$  is increasing, this indicates that the oncoming human driver is conservative. Then the driving style characters mentioned above such as  $d_m$ ,  $d_g$ , etc. will change continuously according to  $M_s$ .

## V. SIMULATION AND RESULTS

The proposed framework is tested at an intersection simulation scenario with various kinds of traffic participants to test the feasibility and evaluate the performance of the framework. It is assumed that the ego vehicle have perfect perception information from the surrounding traffic participants, including the speed, position, acceleration, etc. However, the driving-behaviour character (driving style) is unknown.

Before the simulation starts, the driving characteristics of each human traffic participant as well as the autonomous vehicle are defined through (3). To consider more realistic driving behaviours during intersection left turns, the parameters are set as closely as possible with real-world traffic rules and naturalistic driving behaviours. For example, the maximum speed is extracted from the traffic rule and regulations, minimum time gap are defined through human driving behaviours extracted from real-world driving data in section IV-A.

Table I demonstrates the applied parameters' intervals, which are the minimum distance the minimum time gap and the nominal speed. The features are designed in a continuous way. The word "Neutral" here does not mean purely neutral but indicates that the driver is "in-between" the most aggressive and conservative styles.

Finally, the ratio parameters  $K^*$  can also represent various driving behaviours, however, they are implicitly presented in driving data and would be very difficult to find the exact values that represent fully natural driving characters. Therefore, these parameters are defined through common knowledge and expert driver experience. The safety feature ratios are set to the highest values because safety should be the first priority while driving. The ratios for nominal path and speed cost features are set to smaller values. The ratios for comfort riding features are defined on the smallest scale.

Given the various utility functions representing different traffic participants, the corresponding quadratic approximation

could be obtained by calculating the Hessian matrix and partial derivative vectors ( $L$ ,  $Q$ ,  $R$ ). This transforms the game-based decision making problem into a optimal control problem, and the optimal control policy is proven to be the Nash equilibrium of the game [30]. Thus, by applying the calculated  $L$ ,  $Q$ ,  $R$  into (14) - (18), the Nash equilibrium could be found iteratively, which leads to optimal actions  $\hat{u}_i(k) = \tilde{\gamma}_i^o(k, s(k)) - \delta u_i^*(k)$  of the ego vehicle.

The simulation is operated in a receding horizon format with a 0.25s time step and 5s horizon. In each simulation scenario, the surrounding traffic participants will have a pre-defined driving style that is unknown to the autonomous vehicle. The various driving style of human drivers are represented by behaving differently (more aggressive or conservative) as the autonomous vehicle's expected.

### A. Two Vehicle Interaction Scenario

To evaluate the performance of the proposed framework, a left-turning scenario with only one oncoming vehicle and one left-turning autonomous vehicle is designed. Three kinds of driving styles are tested where all the vehicles start from the same position, speed and initial strategy. The only difference is the driving style of the oncoming vehicles, which is defined by adding a  $\mathcal{N}(0.5, 0.5)$  (aggressive),  $\mathcal{N}(0.0, 0.5)$  (neutral),  $\mathcal{N}(-0.5, 0.5)$  (conservative) on acceleration to the oncoming vehicle at each time step.

The simulation results are shown in Fig. 8. The sub-figures from left to right represent the scenario with aggressive, neutral and conservative oncoming human-driven vehicles. The black lines indicate the boundaries of the road and median strip. The coloured lines indicate the trajectories of the vehicles, whereas the colour indicates the speed of the vehicle along the trajectory. The relation between the speed and colour is indicated in the colour bar on the right. The orange dots along the vehicles' trajectory are time stamps which provide time-state information. The red car in the sub-figures is the autonomous ego vehicle, the blue vehicle is the oncoming vehicle. The light-green-colour arrow at the beginning of the red vehicle's trajectory is the direction of the autonomous vehicle travelling. Finally, the red arrows are the travelling direction of the oncoming human-driven vehicle.

The autonomous vehicles in the sub-figures behave differently when interacting with different human drivers. When interacting with neutral and aggressive human drivers, the autonomous vehicle yield to the oncoming vehicle. Which can be observed by comparing the positions of the two vehicles on the 6th timestamp for Fig. 8 (a) and (b). When cooperating with conservative human drivers, autonomous vehicles drive through the intersection earlier than the oncoming vehicle.

Fig. 8 shows that the proposed framework enables the ego vehicle to adjust its trajectory and speed in different scenarios. The trajectories and speeds of the ego vehicle in Fig. 8 (a) and (b) are different from the ones in Fig. 8 (c). Fig. 8 also presents the different behaviours of various human drivers. The neutral and aggressive human drivers adjust their speed slightly, while the conservative driver decreases their speed before pulling into the intersection.

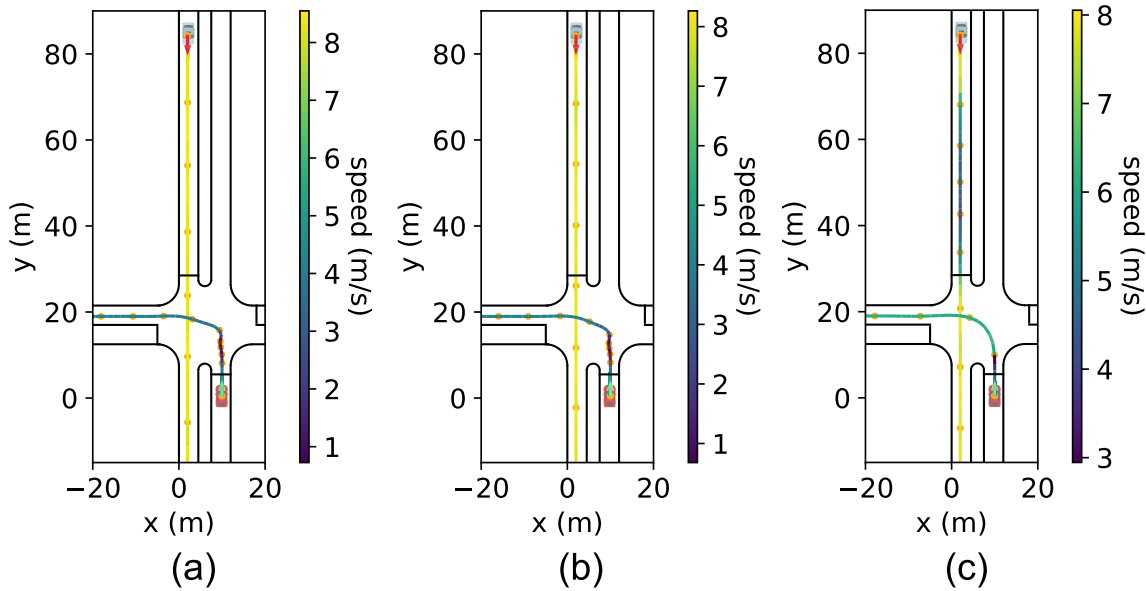


Fig. 8. Typical left-turning scenarios and simulation results.

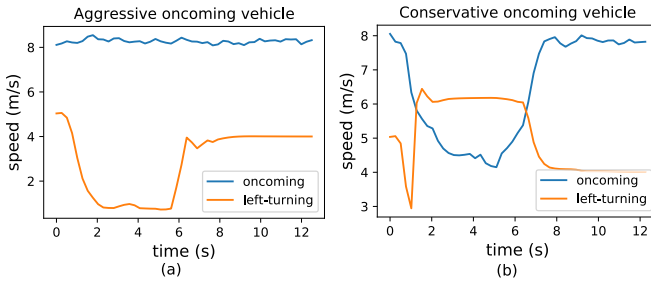


Fig. 9. Speed profiles along trajectories of left-turning and oncoming vehicles in typical left-turning scenarios.

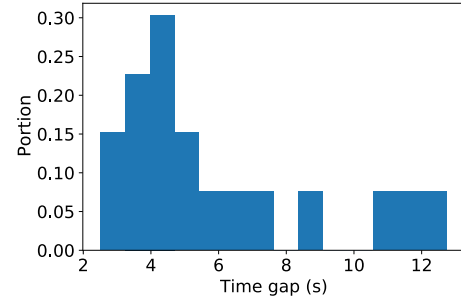


Fig. 10. Accepted time gap distribution in simulation.

The colour bar in Fig. 8 provides a very rough representation of the speed profile along the trajectories of each vehicle. The more detailed speed profiles of the two vehicles are plotted in Fig. 9. Where Fig. 9 (a) and Fig. 9 (b) correspond to the scenario in Fig. 8 (a) and Fig. 8 (c). Which are the scenarios with aggressive and conservative vehicles accordingly.

The blue and orange lines are the speed of the oncoming vehicle and autonomous vehicle respectively. When interacting with the aggressive human driver, the left-turning autonomous vehicle estimates the human driver's behaviour in real-time, then decrease its speed and yield to the oncoming traffic accordingly. When interacting with more conservative human drivers, the ego vehicle increases its speed and tries to pass the intersection as quickly as possible, before getting back to its normal driving speed at intersections.

From these results, the proposed framework is shown to be able to properly interact with various types of human drivers. At the same time, estimates the aggressiveness of the surrounding vehicle and interact with them accordingly. Another feature of the proposed framework is also tested, which is how similar dose autonomous vehicles behave like experienced human drivers. One of the key features that influence the riding experience as well as the receptivity of the surrounding human drivers is the accepted time gap that the left-turning

vehicle takes. Similar scenarios as scenarios in Fig. 8 were tested in simulation with various initial speeds and positions. The scenarios where the left-turning vehicle pulls through the intersection first were extracted, where the TTC is calculated and presented as the histogram shown in Fig. 10.

The x-axis represents the TTC, and the y-axis represents the frequency of the corresponding TTC. From the figure, it can be seen that in most of the interactive scenarios, the left-turning vehicle takes a time gap of around 4.5s. The real-world driving TTC distribution presented in Fig. 6 shows that the left bound is around 5s.

The major difference between the simulation and real-world driving behaviour is due to the intensity of the scenario. The recorded dataset has various kinds of scenarios where the oncoming lane is very empty. In our testing simulations, the scenarios were set to be much more interactive, which might not be very common in the real world. Therefore, the simulation results have larger portions over the 5s side and fewer portions over the 10s side. However, the simulation results of the accepted gap lie within the range of real-world driving data, which shows that the autonomous vehicle is able to perform like humans in this aspect. To evaluate the effectiveness of our proposed framework in enabling the

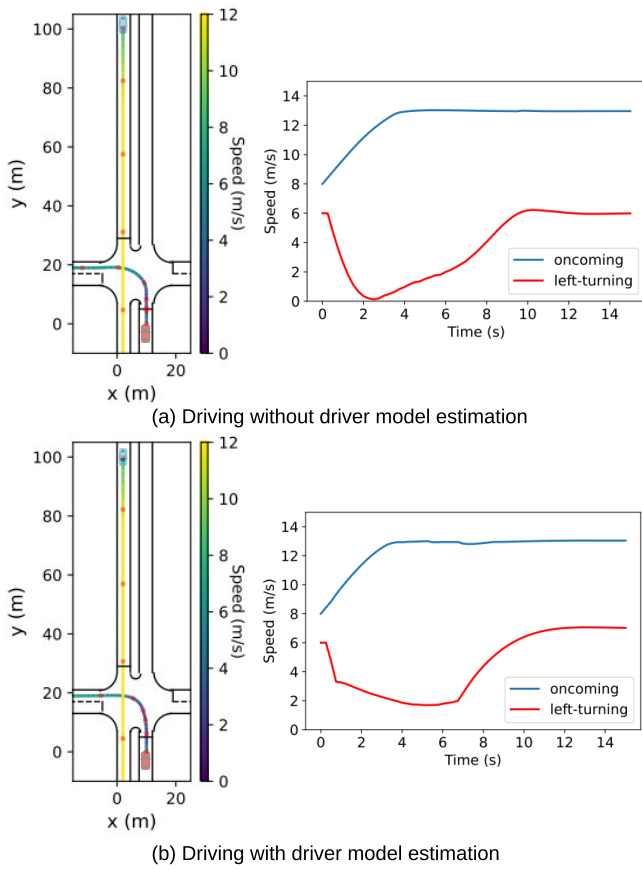


Fig. 11. Comparison between proposed framework with a baseline method.

autonomous vehicle to make sound decisions considering various driving characteristics, a comparison experiment has been done between our proposed method and a baseline decision-making framework that considers a uniform driver model while making decisions.

The testing scenario is selected as a left-turning autonomous vehicle interacting with a conservative oncoming human-driven vehicle and the results are presented in Fig. 11. Fig. 11(a) and Fig. 11(b) represent the baseline and our proposed framework accordingly.

Trajectories of the vehicles of each scenario are presented on the left of Fig. 11, the colour indicates the speed, and the dots are the time stamps. More specific speed profiles are presented on the right. The testing result shows that when dealing with drivers other than neutral drivers, the proposed framework enables the ego vehicle to adapt appropriately to the surrounding driver. At the same time, it maintains a higher speed to ensure higher travel efficiency while keeping a safe distance from human-driven vehicles.

#### B. Two Vehicles and a Pedestrian Interaction Scenario

The framework is also tested in an intersection scenario with both oncoming vehicles and pedestrians. Which is demonstrated in Fig. 12 (a). The blue pedestrian icon is the starting point of the pedestrian and the pink arrow indicates the direction that the pedestrian is walking at.

All the vehicles in the new pedestrian-evolved scenario have a similar starting position and speed as the scenario in Fig. 8.

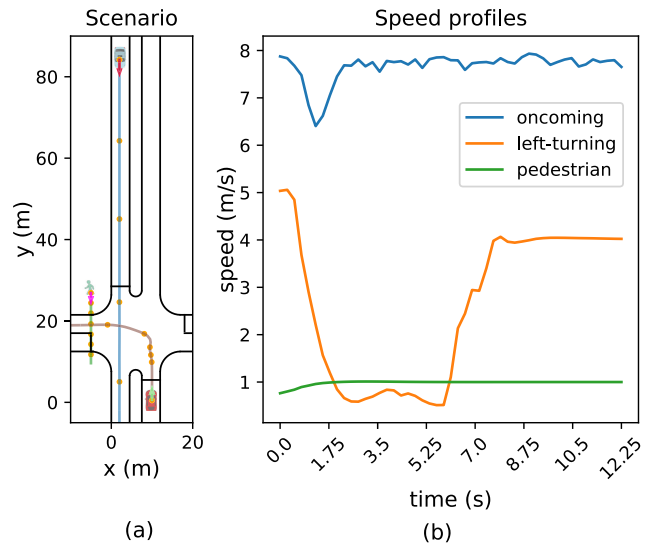


Fig. 12. Scenario simulation result of left-turning at a intersection with the presence of human-driven vehicle and pedestrians.

While the driving style is the same as the one in Fig. 8 (c). The pedestrian is set to cross the intersection with a nominal speed of 1 m/s and a minimum safety gap of 3 m. Without the loss of generality, the human driver's driving style is neutral, and all the pedestrians are set with a static driving style. The trajectories of the traffic participants are plotted in Fig. 12 (a), with time information as time stamps (orange dots) along the trajectory. The trajectories for the autonomous vehicle (red), human-driven vehicle (blue) and pedestrians are represented as orange, blue and green lines accordingly.

From Fig. 8 (c) and Fig. 12 (a) it can be found in a scenario with conservative drivers and no pedestrians, the left-turning vehicle makes the left turn before the oncoming vehicle. However, in the same scenario with a pedestrian, the autonomous vehicle yield to the oncoming vehicle due to the left-turning path was temporarily blocked by the pedestrian.

A more detailed speed profile of each traffic participant could be found in Fig. 12 (b) where the colour of the speed profiles match the colour of the trajectories. It could be found that the conservative human driver decreases its speed first, while the autonomous vehicle also decreases the speed too to yield to the pedestrian and the oncoming vehicle. Then the oncoming vehicle feels safe and pulls through the intersection at its nominal speed. The pedestrian, on the other hand, tries to increase the speed and pass as quickly as possible. The simulation results show that the autonomous vehicle is able to consider the interaction with both drivers and pedestrians. The real-time performance of the decision-making algorithm is also tested. The computational time used for each time step is recorded at each simulation. The computational time over the length of one single time step is calculated and its distribution is presented in Fig. 13. This figure shows that in most of the cases, the algorithm is able to use less than 10% of the time in one time cycle, and in severe cases, still be able to operate in real-time. Thus, the simulation results show that the proposed framework is feasible in real-world application with respect to timing perspective. It is also worth

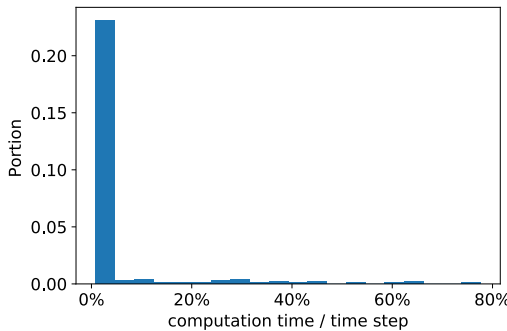


Fig. 13. Real-time performance evaluation.

noting that though the simulation scenarios are autonomous vehicles making left turns, the proposed framework could also be applied in other operating conditions, such as right-turning scenarios by modifying the autonomous vehicle's nominal path and speed profile in the decision-making process.

## VI. CONCLUSION

We proposed a game-theory-based intersection handling method considering the presence of traffic participants with different driving styles. The autonomous vehicle is able to properly estimate the driving style of a human driver and then interact with it accordingly. The simulation results show that the autonomous vehicle's behaviour is close to real-world drivers, which shows that the interaction modelling as well as the driving style estimation works accordingly. Also, the framework is able to operate in real-time which increases the feasibility of the proposed framework.

The proposed framework is able to find a Nash equilibrium (optimal solution) of the formulated decision-making game in real time in most cases. However, finding the global Nash equilibrium is challenging for differential games, and it cannot be guaranteed [20]. One reason for this is that the linear approximation may not hold if the new iterated states deviate too much from the previous states. Therefore, our future work will focus on improving the framework to better preserve the linearity and guarantee that the vehicle finds a Nash equilibrium. One possible solution is to implement a planner before solving the game, which can help decrease the deviation of the states' offsets and improve the accuracy of the solution.

## REFERENCES

- [1] K. Shu et al., "Autonomous driving at intersections: A behavior-oriented critical-turning-point approach for decision making," *IEEE/ASME Trans. Mechatronics*, vol. 27, no. 1, pp. 234–244, Feb. 2022.
- [2] K. Shu et al., "Autonomous driving at intersections: A critical-turning-point approach for left turns," in *Proc. IEEE 23rd Int. Conf. Intell. Transp. Syst. (ITSC)*, Sep. 2020, pp. 1–6.
- [3] M. S. Shirazi and B. T. Morris, "Looking at intersections: A survey of intersection monitoring, behavior and safety analysis of recent studies," *IEEE Trans. Intell. Transp. Syst.*, vol. 18, no. 1, pp. 4–24, Jan. 2017.
- [4] Y. Wiseman, "Autonomous vehicles," in *Research Anthology on Cross-Disciplinary Designs and Applications of Automation*. Hershey, PA, USA: IGI Global, 2022, pp. 878–889.
- [5] S. Li, K. Shu, C. Chen, and D. Cao, "Planning and decision-making for connected autonomous vehicles at road intersections: A review," *Chin. J. Mech. Eng.*, vol. 34, no. 1, pp. 1–18, Dec. 2021.
- [6] S. Li, K. Shu, Y. Zhou, D. Cao, and B. Ran, "Cooperative critical turning point-based decision-making and planning for CAVH intersection management system," *IEEE Trans. Intell. Transp. Syst.*, vol. 23, no. 8, pp. 11062–11072, Aug. 2022.
- [7] T. Fernando, S. Denman, S. Sridharan, and C. Fookes, "Deep inverse reinforcement learning for behavior prediction in autonomous driving: Accurate forecasts of vehicle motion," *IEEE Signal Process. Mag.*, vol. 38, no. 1, pp. 87–96, Jan. 2021.
- [8] G. Li et al., "Deep reinforcement learning enabled decision-making for autonomous driving at intersections," *Automot. Innov.*, vol. 3, no. 4, pp. 374–385, Dec. 2020.
- [9] W. Hu et al., "A rear anti-collision decision-making methodology based on deep reinforcement learning for autonomous commercial vehicles," *IEEE Sensors J.*, vol. 22, no. 16, pp. 16370–16380, Aug. 2022.
- [10] P. Hang, C. Lv, Y. Xing, C. Huang, and Z. Hu, "Human-like decision making for autonomous driving: A noncooperative game theoretic approach," *IEEE Trans. Intell. Transp. Syst.*, vol. 22, no. 4, pp. 2076–2087, Apr. 2021.
- [11] A. Turnwald, D. Althoff, D. Wollherr, and M. Buss, "Understanding human avoidance behavior: Interaction-aware decision making based on game theory," *Int. J. Social Robot.*, vol. 8, no. 2, pp. 331–351, Apr. 2016.
- [12] N. Li, Y. Yao, I. Kolmanovsky, E. Atkins, and A. R. Girard, "Game-theoretic modeling of multi-vehicle interactions at uncontrolled intersections," *IEEE Trans. Intell. Transp. Syst.*, vol. 23, no. 2, pp. 1428–1442, Feb. 2022.
- [13] Y. Rahmati, M. K. Hosseini, and A. Talebpour, "Helping automated vehicles with left-turn maneuvers: A game theory-based decision framework for conflicting maneuvers at intersections," *IEEE Trans. Intell. Transp. Syst.*, vol. 23, no. 8, pp. 11877–11890, Aug. 2022.
- [14] K. Liu, N. Li, H. E. Tseng, I. Kolmanovsky, and A. Girard, "Interaction-aware trajectory prediction and planning for autonomous vehicles in forced merge scenarios," 2021, *arXiv:2112.07624*.
- [15] M. Bouton, A. Nakhaei, K. Fujimura, and M. J. Kochenderfer, "Cooperation-aware reinforcement learning for merging in dense traffic," in *Proc. IEEE Intell. Transp. Syst. Conf. (ITSC)*, Oct. 2019, pp. 3441–3447.
- [16] S. Karimi and A. Vahidi, "Receding horizon motion planning for automated lane change and merge using Monte Carlo tree search and level- $K$  game theory," in *Proc. Amer. Control Conf. (ACC)*, Jul. 2020, pp. 1223–1228.
- [17] S. Pruekprasert, X. Zhang, J. Dubut, C. Huang, and M. Kishida, "Decision making for autonomous vehicles at unsignalized intersection in presence of malicious vehicles," in *Proc. IEEE Intell. Transp. Syst. Conf. (ITSC)*, Oct. 2019, pp. 2299–2304.
- [18] N. Li, I. Kolmanovsky, A. Girard, and Y. Yildiz, "Game theoretic modeling of vehicle interactions at unsignalized intersections and application to autonomous vehicle control," in *Proc. Annu. Amer. Control Conf. (ACC)*, Jun. 2018, pp. 3215–3220.
- [19] P. Hang, C. Huang, Z. Hu, and C. Lv, "Driving conflict resolution of autonomous vehicles at unsignalized intersections: A differential game approach," *IEEE/ASME Trans. Mechatronics*, vol. 27, no. 6, pp. 5136–5146, Dec. 2022.
- [20] D. Fridovich-Keil, E. Ratner, L. Peters, A. D. Dragan, and C. J. Tomlin, "Efficient iterative linear-quadratic approximations for nonlinear multi-player general-sum differential games," in *Proc. IEEE Int. Conf. Robot. Autom. (ICRA)*, May 2020, pp. 1475–1481.
- [21] D. Fridovich-Keil, V. Rubies-Royo, and C. J. Tomlin, "An iterative quadratic method for general-sum differential games with feedback linearizable dynamics," in *Proc. IEEE Int. Conf. Robot. Autom. (ICRA)*, May 2020, pp. 2216–2222.
- [22] H. Xu, Y. Gao, F. Yu, and T. Darrell, "End-to-end learning of driving models from large-scale video datasets," in *Proc. IEEE Conf. Comput. Vis. Pattern Recognit. (CVPR)*, Jul. 2017, pp. 3530–3538.
- [23] J. Peng, Y. Guo, R. Fu, W. Yuan, and C. Wang, "Multi-parameter prediction of drivers' lane-changing behaviour with neural network model," *Appl. Ergonom.*, vol. 50, pp. 207–217, Sep. 2015.
- [24] K. Kreutz and J. Eggert, "Analysis of the generalized intelligent driver model (GIDM) for uncontrolled intersections," in *Proc. IEEE Int. Intell. Transp. Syst. Conf. (ITSC)*, Sep. 2021, pp. 3223–3230.
- [25] S. Albeaik et al., "Limitations and improvements of the intelligent driver model (IDM)," *SIAM J. Appl. Dyn. Syst.*, vol. 21, no. 3, pp. 1862–1892, Sep. 2022.
- [26] Q. Xin, R. Fu, W. Yuan, Q. Liu, and S. Yu, "Predictive intelligent driver model for eco-driving using upcoming traffic signal information," *Phys. A, Stat. Mech. Appl.*, vol. 508, pp. 806–823, Oct. 2018.

- [27] W. Zhan et al., "INTERACTION dataset: An international, adversarial and cooperative motion dataset in interactive driving scenarios with semantic maps," 2019, *arXiv:1910.03088*.
- [28] F. R. Faye, "Modelling of driver's gap acceptance for evaluation of traffic flow characteristics at unsignalized intersection in urban area, Ethiopia," *Amer. J. Traffic Transp. Eng.*, vol. 5, no. 5, pp. 57–64, 2020.
- [29] F. Grognard, R. Sepulchre, and G. Bastin, "Global stabilization of feedforward systems with exponentially unstable Jacobian linearization," *Syst. Control Lett.*, vol. 37, no. 2, pp. 107–115, Jun. 1999.
- [30] T. Başar and G. J. Olsder, *Dynamic Noncooperative Game Theory*. Philadelphia, PA, USA: SIAM, 1998.



**Keqi Shu** (Graduate Student Member, IEEE) received the B.Sc. degree from Northwestern Polytechnical University, Xi'an, Shaanxi, China, and the master's degree in mechanical and mechatronics engineering with the University of Waterloo, ON, Canada, where he is currently pursuing the Ph.D. degree in mechanical and mechatronics engineering. His research interests include interactive planning and decision-making of autonomous vehicles.



**Reza Valiollahi Mehrizi** received the M.Sc. and Ph.D. degrees in statistics from the University of Waterloo, ON, Canada, in 2017 and 2021, respectively. He is currently employed as a Data Scientist and a Statistical Researcher with the Mechatronic Vehicular System Laboratory, University of Waterloo. His research interests include building and developing predictive models using machine learning methods, deep learning object detection and semantic image segmentation, experimental designs, and survival analysis.



**Shen Li** (Member, IEEE) received the Ph.D. degree from the University of Wisconsin Madison, Madison, WI, USA, in 2018. He is currently a Research Associate with Tsinghua University, Beijing, China. His research interests include intelligent transportation systems, architecture design of CAVH system, vehicle-infrastructure cooperative planning and decision method, traffic data mining based on cellular data, and traffic operations and management.



**Mohammad Pirani** (Member, IEEE) received the B.Sc. degree in mechanical engineering from the Amirkabir University of Technology in 2011 and the M.A.Sc. degree in electrical and computer engineering and the Ph.D. degree in mechanical and mechatronics engineering from the University of Waterloo in 2014 and 2017, respectively. He held a post-doctoral researcher positions with the KTH Royal Institute of Technology, Sweden, from 2018 to 2019, and the University of Toronto from 2019 to 2021. He is currently a Research Assistant Professor with the Department of Mechanical and Mechatronics Engineering, University of Waterloo. His research interests include resilient and fault-tolerant control, networked control systems, and multi-agent systems.



**Amir Khajepour** (Senior Member, IEEE) is currently a Professor of mechanical and mechatronics engineering with the University of Waterloo, Waterloo, ON, Canada, where he is also with the Canada Research Chair of mechatronic vehicle systems. He has developed an Extensive Research Program that applies his expertise in several key multidisciplinary areas. He is a fellow of the Engineering Institute of Canada, the American Society of Mechanical Engineers, and the Canadian Society of Mechanical Engineering.